

Silicon microring resonators with 1.5- μm radius

Qianfan Xu, David Fattal, and Raymond G. Beausoleil

Hewlett-Packard Labs, 1501 Page Mill Road, Palo Alto, CA 94304
qianfan.xu@hp.com

Abstract: We demonstrate a junction between a silicon strip waveguide and an ultra-compact silicon microring resonator that minimizes spurious light scattering and increases the critical dimensions of the geometry. We show cascaded silicon microring resonators with radii around 1.5 μm and effective mode volumes around 1.0 μm^3 that are critically coupled to a waveguide with coupled Q 's up to 9,000. The radius of 1.5 μm is smaller than the operational wavelength, and is close to the theoretical size limit of the silicon microring ring resonator for the same Q . The device is fabricated with a widely-available SEM-based lithography system using a stitch-free design based on a U-shaped waveguide.

©2008 Optical Society of America

OCIS codes: (130.3120) Integrated optics devices; (230.5750) Resonators.

References and links

1. A. W. Fang, H. Park, O. Cohen, R. Jones, M. J. Paniccia, and J. E. Bowers, "Electrically pumped hybrid AlGaInAs-silicon evanescent laser," *Opt. Express* **14**, 9203-9210 (2006).
2. A. W. Fang, R. Jones, H. Park, O. Cohen, O. Raday, M. J. Paniccia, and J. E. Bowers, "Integrated AlGaInAs-silicon evanescent race track laser and photodetector," *Opt. Express* **15**, 2315-2322 (2007).
3. W. Bogaerts, D. Taillaert, P. Dumon, D. Van Thourhout, R. Baets, and E. Pluk, "A polarization-diversity wavelength duplexer circuit in silicon-on-insulator photonic wires," *Opt. Express* **15**, 1567-1578 (2007).
4. S. Xiao, M. H. Khan, H. Shen, and M. Qi, "A highly compact third-order silicon microring add-drop filter with a very large free spectral range, a flat passband and a low delay dispersion," *Opt. Express* **15**, 14765-14771 (2007).
5. M. S. Nawrocka, T. Liu, X. Wang, and R. R. Panepucci, "Tunable silicon microring resonator with wide free spectral range," *Appl. Phys. Lett.* **89**, 071110 (2006).
6. A. Liu, R. Jones, L. Liao, D. Samara-Rubio, D. Rubin, O. Cohen, R. Nicolaescu, and M. Paniccia, "A high-speed silicon optical modulator based on a metal-oxide-semiconductor capacitor," *Nature* **427**, 615-618 (2004).
7. Q. Xu, B. Schmidt, S. Pradhan, and M. Lipson, "Micrometre-scale silicon electro-optic modulator," *Nature* **435**, 325-327 (2005).
8. Y. Kuo, Y. Lee, Y. Ge, S. Ren, J. E. Roth, T. I. Kamins, D. A. B. Miller, and J. S. Harris, "Strong quantum-confined Stark effect in germanium quantum-well structures on silicon," *Nature* **437**, 1334-1336 (2005).
9. O.I. Dosunmu, D. D. Cannon, M. K. Emsley, L. C. Kimerling, and M. S. Unlu, "High-speed resonant cavity enhanced Ge photodetectors on reflecting Si substrates for 1550-nm operation," *IEEE Photon. Technol. Lett.* **17**, 175-177 (2005).
10. Q. Xu, S. Manipatruni, B. Schmidt, J. Shakya, and M. Lipson, "12.5 Gbit/s carrier-injection-based silicon micro-ring silicon modulators," *Opt. Express* **15**, 430-436 (2007).
11. Q. Xu, B. Schmidt, J. Shakya, and M. Lipson, "Cascaded silicon micro-ring modulators for WDM optical interconnection," *Opt. Express* **14**, 9431-9435 (2006).
12. P. Rabiei, W. H. Steier, C. Zhang, and L. R. Dalton, "Polymer Micro-Ring Filters and Modulators," *J. Lightwave Technol.* **20**, 1968 (2002).
13. K. K. Lee, D. R. Lim, H.-C. Luan, A. Agrawal, J. Foresi, and L. C. Kimerling, "Effect of size and roughness on light transmission in a Si/SiO₂ waveguide: experiments and model," *Appl. Phys. Lett.* **77**, 1617-1619 (2000).
14. Y. A. Vlasov and S. J. McNab, "Losses in single-mode silicon-on-insulator strip waveguides and bends," *Opt. Express* **12**, 1622-1631 (2004).
15. J. Niehusmann, A. Vörckel, P. H. Bolivar, T. Wahlbrink, and W. Henschel, "Ultrahigh-quality-factor silicon-on-insulator microring resonator," *Opt. Lett.* **29**, 2861-2863 (2006).

1. Introduction

To satisfy the extraordinary interconnect requirements of many-core chips during the next decade, a massively parallel photonic network has to be built on-chip. Recent developments in CMOS-compatible integrated optoelectronic components, including lasers [1,2], filters [3-5], modulators[6-8], and photodetectors [9] have been very promising. However, the high integration density and low power consumption necessary for such a photonic network requires optical devices with even smaller dimensions than that have been demonstrated to date. The silicon microring resonator is a popular choice for such an application because it has small size, high quality factor Q , transparency to off-resonance light, and no intrinsic reflection. The silicon microring resonator can act as an optical filter [4,5], and it can be made into electro-optical modulators [7,10,11], lasers [2] and detectors when carrier injection, optical gain or optical absorption mechanisms are incorporated. This list includes almost all of the optical devices required for the on-chip photonic network.

While a smaller size is universally desirable for most applications of microring resonators for similar reasons, here we concentrate on electro-optical modulation and summarize the benefits of small size on microring modulators. Compact and high-speed electro-optic modulators based on silicon microring resonators have been demonstrated experimentally [7,10]. Microring modulators with different resonant wavelengths can be cascaded to form a wavelength-division multiplexing (WDM) modulation system [11]. For such modulators, a small size is critical for several reasons. First, a smaller size means that more modulators can be fit into a given area, therefore providing higher integration density. Second and more importantly, the power consumption of the modulator, which is a key performance factor for the electro-optical modulators, is directly proportional to the circumference and inversely proportional to the optical quality factor Q of the microring resonator. Reducing the size of the ring without sacrificing the Q is critical for low-power operation. Thirdly, the total bandwidth of the microring-based WDM modulation system [11] is limited by the free-spectral range (FSR) of the microring resonator, which is inversely proportional to the circumference of the ring. A smaller microring modulator has a larger FSR, which can fit in more wavelength channels and have higher aggregated data bandwidth. Given the tremendous benefits of a small size for optoelectronic devices based on the microring resonator, our goal here is to show the lower limit for the size of a high- Q silicon microring.

2. The minimal radius for microring resonators

The microring resonator is formed by tightly bent silicon-on-insulator (SOI) strip waveguide [13,14]. The optical mode in a bent dielectric waveguide is always a leaky mode, with a bending loss that increases as the bending radius decreases. Therefore, at a given resonant wavelength, a microring resonator with a smaller radius will have a lower intrinsic Q .

The black squares in Fig. 1 show the relationship between the radius (measured to the center of the waveguide) and the intrinsic Q of the ring obtained from a 3D finite-difference time-domain (FDTD) simulation. In the simulation, we choose a waveguide with a rectangular cross-section of $450 \text{ nm} \times 250 \text{ nm}$, which is close to the maximal dimension for a single-mode SOI strip waveguide for the quasi-TE mode at a wavelength around $1.55 \mu\text{m}$. The silicon ring is fully surrounded by silicon dioxide. The simulated radii are chosen so that the resonant wavelengths are within $1546.0 \pm 2.2 \text{ nm}$. The data points in Fig. 1 can be fitted very well with a straight line (the dashed line in Fig. 1) on the log-linear scale, showing that the intrinsic Q of a microring resonator increases exponentially with radius of the ring. The intrinsic Q approximately doubles for each $0.1\text{-}\mu\text{m}$ increase in radius. The bending loss of the ring is inversely proportional to the intrinsic Q [11] and is shown on the right y axis in Fig. 1.

To determine the minimal radius for a particular application, one needs to first determine the optimal Q for that application. When the microring resonator is used as a high-speed modulator, a higher Q is beneficial to reduce power consumption [10], but when the Q is too high, it limits the maximum modulation frequency and causes high temperature sensitivity. For a modulator working at 10–20 Gbit/s, a moderately high operating Q on the order of 10,000, which corresponds to an optical bandwidth of ~ 20 GHz, is appropriate for the critically coupled resonator, which requires an intrinsic Q of 20,000. From Fig. 1, one can conclude that the minimal radius to obtain an intrinsic Q of 20,000 around the wavelength of 1.55 μm is 1.37 μm .

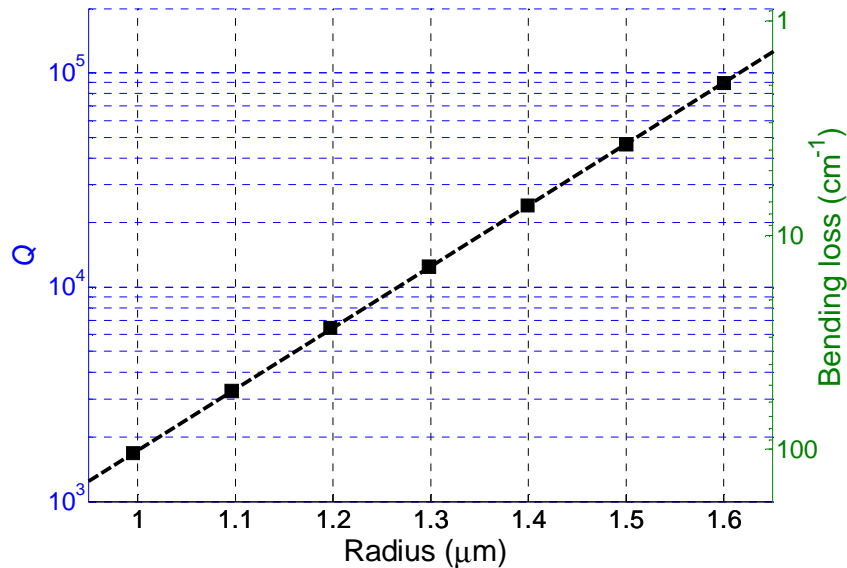


Fig. 1. The optical quality factor Q and waveguide bending loss versus the radius of a microring resonator obtained from a 3D FDTD simulation.

The simulation results shown above only include the fundamental (intrinsic) bending loss. The scattering loss caused by the sidewall roughness will further decrease the Q of the resonator. Therefore, for the following theoretical and experimental work, we choose a slightly larger radius of 1.5 μm , which has an intrinsic Q of 46,600 without sidewall roughness. This higher theoretical value for the intrinsic Q gives some margin for degradation due to scattering loss. The effective mode volume of this 1.5- μm microring resonator is calculated to be only 1.0 μm^3 .

3. Coupling to ultra-compact microring resonators

A microring resonator is normally coupled to a straight waveguide with the same width [7]. It is critically-coupled [15] to the waveguide when the one-pass optical coupling between the ring and the waveguide matches the round-trip optical loss in the ring. For a microring resonator with radius as small as 1.5 μm , it is difficult to obtain the critical coupling due to the extremely short interaction length. In order to be critically coupled to the waveguide, a microring resonator with 1.5- μm radius and an intrinsic Q of 20,000 should have a 0.8% one-pass power coupling coefficient to the waveguide. Even though the coupling strength needed is relatively low, it still requires a narrow gap between the ring and the waveguide, due to the short interaction length and the high confinement nature of the waveguides. The small gap is not only difficult to fabricate, but also dramatically increases the optical loss and reduces the Q of the ring [16], as we will show next.

To investigate the single-pass optical coupling between a straight waveguide and the bent waveguide forming the ring, we ran a 3D FDTD simulation on the structure shown in Fig. 2(a), where the outlines of the waveguides are shown in gray. The field has a quasi-TE polarization and is launched relatively far from the coupler and sent to the curved waveguide (having a radius of 1.5 μm) using a section of horizontal waveguide, and is then partially coupled into the vertical waveguide. Both the straight and the curved waveguides have a rectangular cross-section of 450 nm \times 250 nm, and the wavelength is 1.55 μm . The color scale image in Fig. 2(a) is a snap shot of the H_z component at the central plane of the waveguides.

One can see from Fig. 2(a) that the modes in the straight waveguide and the curved waveguide are not well phase-matched. Because the tightly bent waveguide breaks the symmetry in the coupling region, the phase matching condition is no longer satisfied between waveguides with identical dimensions. The phase mismatch not only reduces the coupling efficiency, but also creates higher-order mode components, which distort the fields in the straight waveguide. These higher-order components will eventually radiate to the environment as it propagates along the straight waveguide, since the waveguide can only guide the fundamental mode. Therefore, the coupling to the higher-order component will create an additional source of radiation loss for the ring, and degrade the intrinsic Q of the microring resonator, which makes it even harder to achieve critical coupling. In the fabricated devices, the Q 's of 1.5- μm -radius microring resonators critically coupled to a waveguide with the same width of 450 nm are consistently measured below 3,000. In order to be critically couple to the ring with the lower intrinsic Q , the gap between the waveguide and the ring needs to be reduced to ~ 100 nm, which is hard to fabricate and to control precisely.

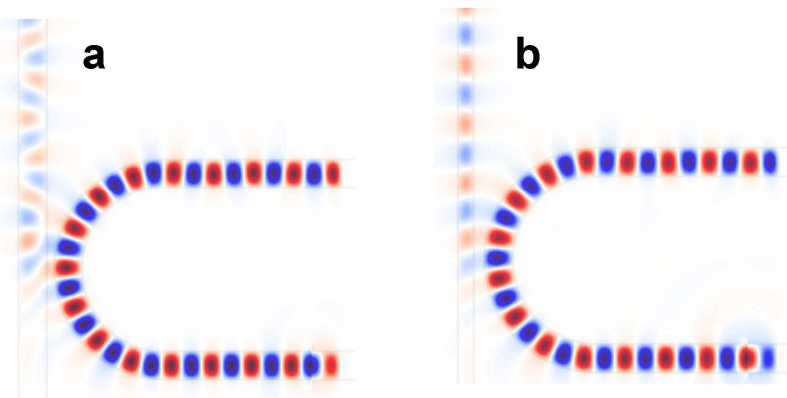


Fig. 2. FDTD simulated field coupling from a curved waveguide with 1.5- μm radius to a straight waveguide at the wavelength of 1.55 μm . The plotted field component is H_z at the central plane of the waveguide and the ring. Deeper red means more positive field and deeper blue means more negative field. (a): both straight and bent waveguides are 450-nm wide. The gap between them is 100 nm. (b) the straight waveguide is 250-nm wide and the bent waveguide is 450-nm wide, with a 200 nm gap between them

Figure 2(a) shows that the mode of the curved waveguide extends concentrically at the outward side. Since the straight waveguide is farther from the center, one can speculate that if the mode of the straight waveguide had a longer spatial period, it would have a better phase match with the concentric mode in the tightly curved waveguide. A waveguide mode with longer spatial period needs to have a lower effective index, which can be obtained by reducing the width of the waveguide. Figure 2(b) shows the optical field when light couples from the curved waveguide to a straight waveguide with a reduced width of 250 nm and a lower effective index of 1.7 for the quasi-TE mode, compared to the effective index of 2.5 in

the 450-nm-wide waveguide. One can see from the Fig. 2(b) that the mode in the narrower waveguide with longer spatial period has a better phase match with the concentric mode in the curved waveguide, and much weaker higher-order components are excited, which is evident from the symmetry of the field in the straight waveguide.

In addition, the mode of the narrower waveguide decays more slowly in the cladding because of the lower effective index. Therefore, it has a higher mode overlap with the adjacent ring, and the gap between the ring and the waveguide can be *increased*. With the 250 nm wide waveguide, we can obtain the desired 0.8% power coupling with a gap of over 400 nm according to the FDTD simulation. The larger gap is much easier to fabricate and to control, and all the critical dimensions of the device are well within the reach of optical lithography.

Another possible way of increasing the optical coupling coefficient between the waveguide and the ring is to add a straight section in the coupling region of the ring and form a racetrack structure [16]. This approach, however, will dramatically reduce the intrinsic Q of the resonator because of the mode mismatch between the straight and tightly curved sections of the racetrack waveguide, since the light experiences losses from this mode mismatch four times during each trip around the racetrack structure. A 3D FDTD simulation shows that, when adding a 0.5- μm -long straight waveguide section to a 1.5- μm -radius ring, the intrinsic Q of the resonator drops from 46,600 to below 2,000. Apparently, the racetrack structure is not a good solution to the coupling problem in an ultra-compact resonator.

4. Device design and fabrication

The device is fabricated on a silicon-on-insulator substrate with 3- μm buried oxide using a scanning electron microscope (SEM)-based e-beam lithography system. The pattern is first defined on a layer of negative e-beam resist (Fox-12) by an externally controlled SEM with an accelerating voltage of 30 kV. The pattern is then etched into the silicon layer using an HBr-based reactive ion etching process. The device is then spin-coated with a ~ 2 - μm thick Polymethyl-methacrylate (PMMA) layer in order to match the refractive indices of the upper cladding and lower cladding of the waveguide.

While SEM-based e-beam lithography systems are widely available in most university campuses, they are traditionally viewed as unsuitable for fabricating devices based on sub-micron silicon waveguides. The main reason for this belief is that SEM-based systems cannot precisely stitch the writing fields (normally a few hundred microns wide); therefore any waveguide crossing the boundary of the writing fields will be broken. As a result, most of the experimental works on sub-micron silicon waveguides have been done using dedicated (but very expensive) e-beam writers, where mm-long waveguides can be fabricated by precisely stitching multiple writing fields. The mm-long waveguides are believed to be necessary to run from edge to edge on the chip for optical input and output coupling on both edges.

By contrast, we designed the U-shaped waveguide shown in Fig. 3(b), where the whole length of the waveguide is fitted within one writing field. Since the waveguide never crosses a field boundary, no precise stitching of the field is required. Based on this design, one can fabricate and test silicon nanophotonic devices coupled to sub-micron waveguides using an SEM-based lithography system, which has much lower cost and wider availability in academic institutes than dedicated e-beam writers.

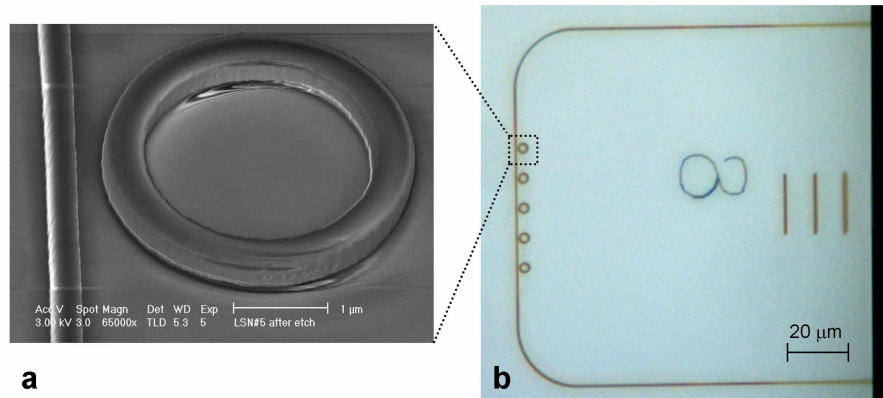


Fig. 3. (a): An SEM picture with 40° tilted view of the microring resonator with 1.5- μm radius coupled to a waveguide with reduced width. (b): A microscope picture of the cascaded microring resonators coupled to a U-shaped waveguide at the edge of the chip.

Figure 3(a) shows an SEM picture of a microring resonator with a radius of 1.5 μm before it was cladded with PMMA. Both the waveguide and the ring have a height of 250 nm and sidewall angle of $\sim 84^\circ$. The waveguide forming the ring has an average width of ~ 440 nm. The straight waveguide coupling to the ring has an average width of ~ 290 nm, and the gap between the waveguide and the ring is ~ 340 nm. The width of the straight waveguide used in the FDTD simulation happens to equal the height of the waveguide. Here, in order to avoid the cross-coupling between the quasi-TE mode and quasi-TM mode in a square waveguide, we increased the width of the straight waveguide. This ring is one of the five rings coupled to the same waveguide, as shown in the top-view microscopic picture in Fig. 3(b). The five rings are designed to have slightly different radius, so that their resonances are uniformly distributed throughout the FSR.

5. Optical measurement setup and results

Figure 4(a) shows the experimental setup for measuring the transmission spectrum of the device. The output of a tunable laser is collimated and focused by a lens onto one end of the U-shaped waveguide. The output light at the other end of the U-shaped waveguide is collimated by the same lens and sent to a detector. A polarizer is placed in front of the detector to separate the quasi-TE and quasi-TM modes.

Figure 4(b) shows the normalized transmission spectrum of the quasi-TE mode. The resonance features from the five microring resonators coupled to the waveguide (see Fig. 3(b)) can be identified on the spectrum. Figure 4(c) shows the spectrum around the second resonance in Fig. 4(b). The FWHM width of the resonance is 0.17 nm, corresponding to a Q of 9,000, close to our target of 10,000. The extinction ratio of the resonance is ~ 16 dB, showing that the ring is close to being critically coupled to the waveguide. Therefore, the intrinsic Q of the ring is about twice the coupled Q , or 18,000. This is lower than the simulated intrinsic Q mainly because of the scattering loss from the sidewall roughness. To estimate the level of scattering loss, we measured an intrinsic Q of $\sim 40,000$ on microring resonators with radii of 2.5 μm , which is primarily due to scattering loss, since the bending loss at this radius (can be estimated by extending the line in Fig. 1) is negligible. If a 1.5- μm -radius ring has the same scattering loss, it would have an intrinsic Q of $\sim 21,500$. The measured Q of the 1.5- μm -radius ring (18,000) is slightly lower than the above calculation, showing that the 1.5- μm -radius ring has a slightly higher scattering loss. This is mainly because the optical spatial mode in a smaller ring shifts more to the outer side of the ring, and therefore has higher overlap with the sidewalls. From the transmission spectrum, the FSR of

the 1.5- μm -radius microring resonator is measured to be 62.5 nm, from which a group index of 4.2 is calculated [11], which agrees well with that measured in similar devices [5].

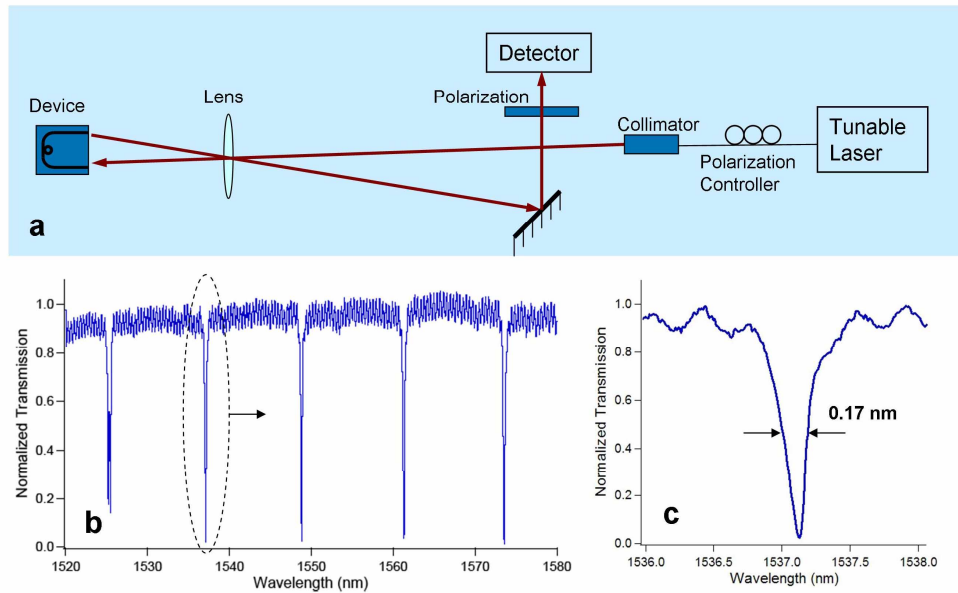


Fig. 4. (a): Schematic of the experimental setup for measuring the transmission spectrum of the device. (b): The transmission spectrum of five cascaded microring resonators, showing the resonant dips from all 5 rings. (c): Zoom-in spectrum around the second resonance in (b).

6. Summary

In conclusion, we have designed a junction between a silicon strip waveguide and an ultra-compact silicon microring resonator that minimizes spurious light scattering and increases the critical dimensions of the geometry. We fabricated a network of compact micro-rings critically coupled to strip waveguides, with ring radii as small as 1.5 μm , and were able to measure a coupled Q of 9,000, close to our target of 10,000. They have smaller radius, larger FSR and higher Q than the previously demonstrated microring resonators [4,5]. Their radii are smaller than the wavelength of light and are close to the theoretical limit of $\sim 1.37 \mu\text{m}$ for the targeted Q . The device fabrication was realized with a widely-available SEM-based lithography system using a stitch-free design based on a U-shaped waveguide. The smallest feature in the design is $\sim 300 \text{ nm}$ in size, which is well within the reach of optical lithography.